ISSN 2007-9737

Computing of the Forward and Inverse Solutions of Electrical Impedance Tomography Using a 32-bit Microcontroller System

Miguel Ángel San-Pablo-Juárez[1,*], Maria Montserrat Oropeza-Saucedo[1], Eduardo Morales-Sánchez[2]

[1] Universidad de las Américas Puebla,
Departamento de Computación, Electrónica y Mecatrónica,
Mexico

[2] Instituto Politécnico Nacional,
Centro de Investigación en Ciencia Aplicada y Tecnología Avanzada, Unidad Querétaro,
Mexico

miguel.sanpablo@ieee.org, maria.oropeza@udlap.mx, emoraless@ipn.mx

Abstract. The forward and inverse solution of the Electrical Impedance Tomography (EIT) governing equation (Laplace's and Poisson's equation) have been analyzed and implemented in personal computers and small board computers but not in computers based on microcontrollers. In this work, both solutions, the forward and inverse problem were computed and implemented into an embedded system based on 32-bit microcontrollers with practical applications as portable tomographic systems avoiding the use of a PC and reducing the size of the tomographic systems, this means that it is not required a PC to compute the forward or inverse solution in EIT.

Keywords. Embedded system, forward solution, inverse problem, electrical impedance tomography.

1 Introduction

When someone wants to build a system for Electrical Impedance Tomography, first must solve the governing equation having two main problems, to find the Forward (Laplace's equation) and Inverse solutions (Poisson's equation). Solving the forward problem corresponds to finding the electrical potential and knowing the conductivity distribution in the body. The inverse problem corresponds to finding a conductivity distribution knowing the body's electrical potentials when applying a current. Both forward and inverse problems have been studied for decades and are well-known in many ways to find solutions [1].

1.1 Electrical Impedance Tomography

Electrical Impedance Tomography (EIT) uses electrodes placed on the surface of a body to make measurements and then an image of the electrical conductivity distribution within the body is reconstructed with an algorithm [2,3]. Compared to the CT scan or MRI scan, EIT offers poor imaging resolution. However, EIT is a radiation-free imaging modality, and it is completely non-invasive as long as the drive current amplitude meets safety standards [4]. Usually, a set of voltage measurements is acquired from the boundaries of a conductive region, applying a sequence of low-frequency current patterns [5]. Most of the EIT authors use a PC for displaying measurements and conductivity distribution as in [6-8], even more, the most common way to show EIT images is through a software called EIDORS. This paper proposes an embedded system to solve the forward and inverse problems in EIT.

1.2 The Forward Problem

The typical *forward problem* in EIT is as follows: Given the conductivity distribution σ and the

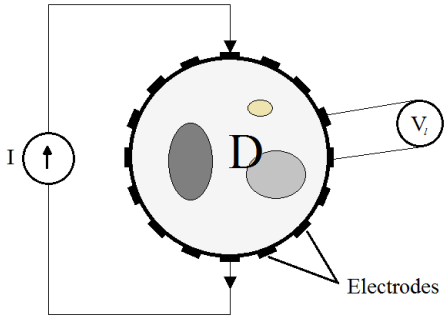

Fig. 1. A typical EIT configuration system with a current source I, potential measurement V, and electrode placement

currents injected through boundary electrodes, *I*, find the potential distribution φ within the object *D* and in particular the resulting voltages at the potential measurement electrodes, V [9]. Figure 1 shows a typical connection of electrodes around an object and the current injection with the potential measurement.

The solution to the forward problem is rather simple as solving the nonlinear governing equation:

$$\nabla \cdot (\sigma \nabla \varphi) = 0, \tag{1}$$

for φ in *D* together with the application of the boundary conditions imposed by the current injection and subsequent determination of the electrode voltages *V* [9].

This equation can be rewritten as an operator equation:

$$Y(\sigma)\, \varphi = J, \tag{2}$$

where *Y(σ)* is known as the conductivity-dependent Dirichlet-to-Neumann map, and *J* is the current density applied trough boundary conditions.

1.3 The Inverse Problem

The *inverse problem* is based on a model identification problem as follows: Given the injected currents *I* (causes) and the corresponding voltages at the potential measurement electrodes *V* (effects), find the conductivity distribution σ (the physical model) within *D.*

In this problem, equation (1) is non-linear in σ, because the potential φ is a function of the conductivity, that is φ = φ(σ):

$$\nabla \cdot \sigma \nabla(\varphi(\sigma)) = J. \tag{3}$$

Equation (3) cannot be solved analytically for arbitrary σ's and thus requires the application of appropriate numerical techniques.

To obtain a numerical solution to the continuous problem, the solution domain needs to be discretized into small finite elements, on which a solution is then approximated.

1.4 Embedded System Using the STM32F Board

A solution to governing equation (1) with an embedded system was studied in [10]. It consists of a microcontroller system that solves numerically Laplace's equation using the Finite Element Method (FEM) with a 32-bit microcontroller electronic board and a screen is used to display results.

In this case, Laplace's equation can be generalized to be solved using the same system with the same methodology. The forward problem can be solved then with the FEM and the board with a microcontroller, the model to be used may be the STM32F746G-DISCO or the STM32F429 Discovery, both boards use programming C language, with the suite STM32CubeIDE.

The inverse problem has been studied widely by EIT experts [11-13], nevertheless in this work is proposed to use the same microcontroller board as an embedded system to solve the inverse problem and display a tomographic image. It can be done using the linear Sheffield back-projection algorithm.

The solution of the inverse problem can be implemented into the microcontroller using linear back-projection implementing the back-projection matrix from [13].

The method produces an image with a resolution of 32x32 pixels in the STM32F429 or 320x320 pixels in the STM32F746G. The image can be filtered to smooth the poor resolution. The method can get numerical values from conductivity σ in each discretized element from region D.

ISSN 2007-9737

2 Materials and Methods

2.1 Implementation

The implementation seeks to test a 32-bit microcontroller system to avoid the use of a personal computer and to give portability to a small and compact tomographic system; the idea is to construct a portable tomographic device later, this is planned to be built using an embedded system by example for vein detection [14] or another application where small electronics or portable EIT system must be used. To test the microcontroller system, a commercial board is used, it consists of the MCU STM32F429ZIT6 Discovery based on the ARM Cortex-M processor; a product that combines high performance, real-time capabilities, digital signal processing and low-power, low-voltage operation and ease of development [15]. In this work, the implementation was programmed in the STM32F746G-DISCO board too. The size of any board is not larger than 108 mm x 80 mm.

The forward solution in EIT is commonly solved by the FEM, where a continuous region is divided into a finite number of discrete elements, that can be triangular or quadrilaterals, and an approximation to a solution of equation (1) is obtained. The potential φ inside all region D is computed. An example of a finite element mesh is shown in Figure 2, with 64 triangular elements in the circular region D. Figure 2 shows the numbering for elements and nodes of the used mesh, the board used only supports meshes from a low number of elements as in this case, for a mesh with a major number of elements it will be necessary to use another microcontroller too powerful.

The methodology implemented in this section is used in [16], but in this case, only the 2D case was taken. A first computing for the forward problem was implemented and the numerical values for potential were computed and shown in the display of the hardware. Figure 3 shows the numerical results computed by the 32-bit ARM microcontroller.

The compiler used was STM32FCubeIDE for ARM. This suite uses C language and supports the libraries for the Discovery platform STM32F429 and STM32F476G. This work may be similar to

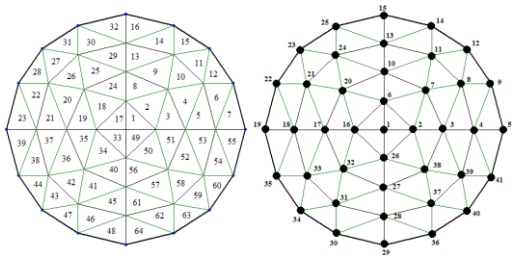

Fig. 2. Finite Element mesh used for this example to solve the forward problem in EIT

Fig. 3. STM32F computing the forward solution in EIT for a 64-element mesh

other systems as [17-19], but the main difference is that in this work, a PC is not required to compute the forward or the inverse problem.

2.2 Inverse Implementation

The Sheffield back-projection from [13] was used. For this case, the following equation satisfies the back-projection reconstruction equation:

where σ is a vector of conductivities in each discrete element, B_M is a back-projection matrix: from [13] and V is the measured voltage between

$$\sigma = B_M \cdot V, \tag{4}$$

electrodes in all projections. In this case, the circular domain was discretized into 32 x 32 pixels, so for this work, we have 16 electrodes around the EIT phantom, and the current injection will be the adjacent configuration, then the equation (4) becomes:

To validate the results, it was taken a typical example from EIDORS software of two objects into an EIT phantom shown in Figure 4. The results in Figure 6 were implemented into the MCU system and the following was observed: The numerical results for the forward problem match and are the

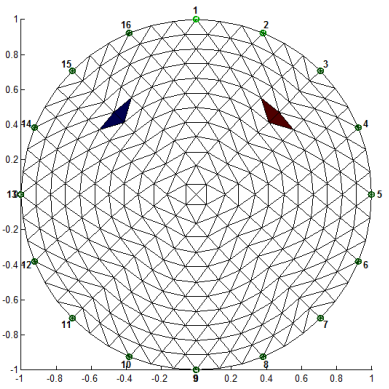

Fig. 4. Example from EIDORS software of two objects in a phantom

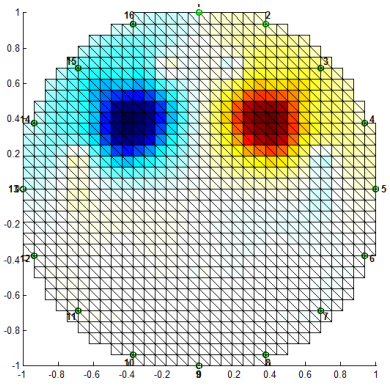

Fig. 5. Back-projection solution using EIDORS

same with no numerical error, but only the results in the inverse problem from the image change, that is because the image displayed into the screen is shown in grayscale, while in the EIDORS example is with a red-blue color scale; because the display of the board can show only colors from ARGB565 or ARGB8888 resolution; the image may be a little bit hard to compare with the EIDORS example, and yet, qualitatively the results agree with the EIDORS one.

$$\sigma_{912x1} = [B_M]_{912x208}[V]_{208x1}, \quad (5)$$

with B_M of size 912x208, because the number of voltage measurements is 16 of 13 pairs; the 912 conductivity values of σ, is because the 32x32 pixels give a total of 1024 values, but the circular domain, only contains 912 pixels inside. So, the relation (5) is used to reconstruct solving 912 values of conductivity.

The voltage to be used is:

$$V = (V_{meas} - V_{ref})/V_{ref}, \quad (6)$$

where V_{meas} is the vector of 208 measured potentials at the boundary of the EIT phantom; Vref is the vector of 208 potentials calculated from the forward solution in a homogeneous medium.

Figure 4 shows an example of two objects in a phantom tank with conductivities of 1.1 and 0.9; after computing to solve the inverse problem in EIDORS the output is observed in Figure 5.

Note that the reconstruction has values from conductivity that show high contrast. The implementation of this algorithm can be shown first clearly, imaging the vector of σ's with their respective values and printing it as in Figure 6.

Figure 6 shows the reconstructed image with the algorithm used in [12] to be implemented into the microcontroller system.

3 Results

Forward and inverse solutions were programmed into an embedded system using the STM32CubeIde compiler. Both solutions were built into the memory of an ARM Cortex M4 and M7 microcontroller from 2 different boards: Discovery STM32F429 and STM32F746G respectively. The best results were made by the STM32F746G board, because the processor got a high speed up to 462 DMIPS and 200 MHz compared with the version of STM32F429 of lower speed at 180 MHz.

Both boards have the inconvenient that the RAM memory needs to be expanded or use external if you want to declare big matrices as the Back-projection Matrix.

In this implementation, the operations only were made between float precision numbers, not in double format because of the specifications of the RAM memory even expanded or using external.

The implementation into the Discovery STM32F was compiled successfully in both forward and inverse problems. The results for the inverse problem are shown in Figure 7. The code was compiled and loaded in both STM32F429 and STM32F746G discovery boards.

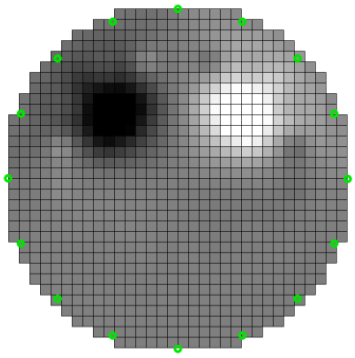

Fig. 6. Back-projection solution using the Sheffield back-projection matrix

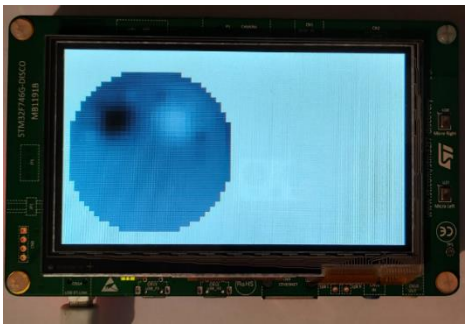

Fig. 7. Output image using Sheffield back-projection and STM32F746G

The RMS error for the forward problem using the FEM was of 1.31E-4, with an R-squared of 1. The maximum absolute error was of 4E-4 V for a 41 nodes and 64 elements mesh, as shown in Figure 2.

The RMS error for the inverse problem was of 12.6E-4 with respect to the computed in the PC with EIDORS, with an R-squared of 0.995, which is due to computing with float data type number, while in the PC the computing is using double data type numbers. Figure 8 shows the absolute error of the conductivity obtained with the STM32F746 board respect the obtained with a PC using EIDORS. The error was measured using the *fitlm*() function in MATLAB software.

Note that exist a small error in all elements of the image of a normalized conductivity map of 912 computed values (represented as pixels) in Figure 8. Figure 8 shows that the error was up to 6.3E-4 S/m.

In this case, the obtained image is shown in the LCD display contained in the development board. The resolution looks poor, but the conductivity map image is too similar to the computed by EIDORS

software. The results are displayed directly without any filter and the contrast is shown normalized to a 104 times conductivity scale, this is because the back-projection matrix is normalized. A result computed in the STM32F429 is shown in Figure 9. The example is the same, but the used board has less RAM and a slower processor than the STM32F746G board. Another characteristic that is useful in the EIT systems is that the board STM32F746G can compute and display the values of the conductivity map (grayscale) into a colormap value, by example, it was probed a colormap with 256 colors, which is shown in the Figure 10.

The processing times for the reconstruction were 1.37 seconds in STM32F429 and 1.02 seconds in STM32F746, compared to a PC-based system with 0.767 seconds of computing. The time was measured with the *HAL_GetTick()* function available on the STM32CubeIDE. The same EIT reconstruction was made with the back-projection method in EIDORS, this system is up to 2 times slower than the PC computed system even when the STM32 used float data, and the PC uses double type data for making operations. The difference in the spent time by the solution between the STM32F429 and STM32F746 is 0.74, which means that the STM32F7 is 0.74 times faster than the STM32F4 system to compute a complete EIT using the back-projection method.

The compiler STM32FCubeIDE built the application in just 1.22 seconds while the uploading to the board spent 15 seconds.

Compilation and execution times are typically higher, compared to other development environments used in PC, such as Matlab, C/C++, or Eclipse, but the upload method is easier and faster compared to a PC application, this is due to the uploading is made using integrated interfaces such as STLink hardware included in the board, which is an interface for fast programming.

Limitations of the system are that this system only computes both solutions for 8 electrodes systems, this is because the computing is oriented for portable and small applications that need getting images of an EIT. Another limitation is that

ISSN 2007-9737

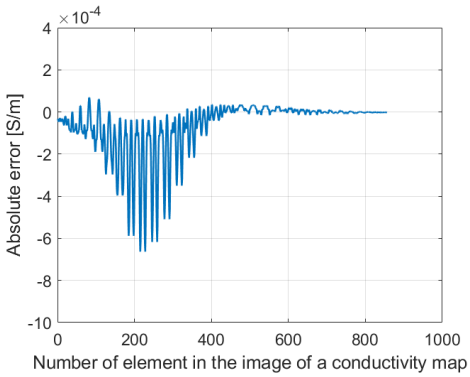

Fig. 8. Comparison of absolute error of a computed EIT with the microcontroller concerning the same computed with a PC

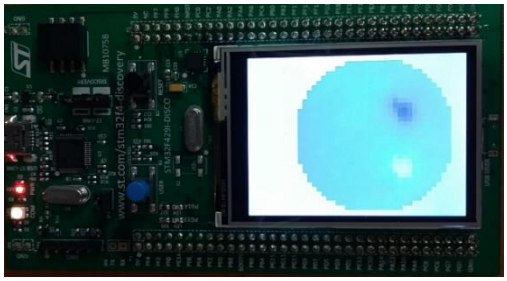

Fig. 9. Implementation of the inverse solution

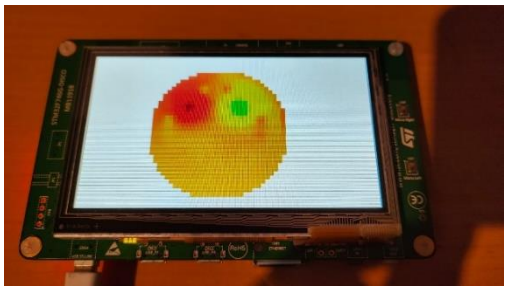

Fig. 10. Colormap example in the board that is useful for computing EIT

the operation voltage is 3.2V, so it is required additional voltage sources for a complete EIT system.

The presented tests were made using only 8 electrodes. The specific application of this design is to compact an EIT system to ensure portability or save space making a tomograph, this is due to the possible applications such as vein detecting or bone density measurement and also corporal composition monitoring. The practical benefits of this implementation for end users are mainly the portability, because it replaces a considerable area, reduces in size of a tomographic system, and avoids the use of a PC, reducing costs in building small prototypes of an EIT system.

The presence of noise was not analyzed in this example because this system only considers the computing of the forward and inverse problem, not the acquiring of potential signals or signal conditioning. Artifacts neither were considered because the probe of both forward and inverse problem were computed using example numerical values taken from EIT data community.

Experimental validations were made only at a simulation level because the whole system does not contain a complete system for acquiring potentials around electrodes, which implies the use of a current source, signal conditioning, a multiplexing matrix, and an in-phase measurement system.

The embedded system computes the forward and inverse problems separately, but it is planned to expand the memory in future works. It is expected that will be possible to compute EIT for systems with more than 8 electrodes and more resolution in terms of pixels displaying in the screen, for improvement with memory expansion, by example using an extra RAM, or ROM as microSD card or EEPROM memories.

4 Conclusions

Both, the forward and the inverse solution to Electrical Impedance Tomography were programmed into an embedded system and a conductivity distribution was reconstructed. The conductivity distribution was shown in a figure of a conductivity map in an LCD contained in the embedded, this shows that it is possible to use a microcontroller for computing EIT using an embedded system, not only a PC.

This implementation can be applied to projects that require low resources and small size, with small components or portability characteristics, this is due to all processing being made into the microcontroller over the board that is embedded into an area of 100 cm2.

Unfortunately, the memory of STM32F boards was not sufficient to compute the reconstruction via back-projection inside the device, because the back-projection matrix takes more memory than expected, but by expanding the RAM the computing was successful.

Acknowledgments

The authors would like to thank to Consejo de Ciencia y Tecnología del Estado de Puebla CONCYTEP for the given funding.

References

1. **Holder, D.S. (2008).** Electrical Impedance Tomography: Methods, History and Applications. Institute of Physics Publishing.
2. **Zhang, X., Xu, G., Zhang, S., Li, Y., Guo, Y., Li, Y., Wang, Y., Yan, W. (2014).** A Numerical Computation Forward Problem Model of Electrical Impedance Tomography Based on Generalized Finite Element Method. IEEE Trans. on Magnetics.
3. **Antink, C.H., Pikkemaat, R., Leonhardt, S. (2013).** A GREIT-type linear reconstruction algorithm for EIT using eigenimages. Journal of Physics. Conference Series.
4. **Bahrani, N., Adler, A. (2012).** 2.5D Finite Element Method for Electrical Impedance Tomography considering the Complete electrode Model. 25th IEEE Canadian Conference on Electrical and Computer Engineering.
5. **Polydorides, N. (2002).** Image Reconstruction Algorithms for Soft-Field Tomography, PhD dissertation. University of Manchester Institute of Science and Technology.
6. **Li, T., Isaacson, D., Newell, J.C., Saulnier, G.J. (2013).** Studies of an Adaptive Kaczmarz Method for Electrical Impedance Imaging. Journal of Physics: Conference Series.
7. **Cheney, M., Isaacson, D., Newell, J.C. (1999).** Electrical Impedance Tomography. SIAM Review, Vol. 41.
8. **Polydorides, N., Lionheart, W.R.B. (2002).** A Matlab toolkit for threedimensional electrical impedance tomography: A contribution to the Electrical Impedance and Diffuse Optical Reconstruction Software project. Measurement Science and Technology.
9. **Molinari, M. (2003).** High Fidelity Imaging in electrical Impedance Tomography. PhD dissertation University of Southampton.
10. **San-Pablo-Juárez, M.A., Morales-Sánchez, E., Ireta-Moreno, F. (2015).** Embedded system to solve the Laplace's Equation. Technological Trends in Computing. Research in Computing Science, Vol. 98, pp. 161–171.
11. **Adler, A., Arnold, J.H., Brown, B., Dixon, P., Faes, T.J.C., Frerichs, I., Gagnon, H., Grber, Y., Grychtol, B., Hahn, G., Lionheart, W.R.B., Malik, A., Patterson, R.P., Stocks, J., Tizzard, A., Weiler, N., Wolf, G.K. (2009).** GREIT: A unified approach to 2D linear EIT reconstruction of lung images. Physiol. Meas, Vol. 30.
12. **Santosa, F., Vogelius, M. (1990).** Backprojection algorithm for electrical impedance imaging, SIAM J. Applied Mathematics, Vol. 50, pp. 216–243.
13. **Barber, D.C., Brown, B.H. (1984).** Applied Potential Tomography. J. Phys. E: Sci. Instrum, Vol. 17, pp. 723–733.
14. **San-Pablo-Juarez, M.A., Orozco-Corona, D.M. (2021).** Method of peripheral vein detection using Electrical Impedance Tomography. J. Phys. Conf. Ser. 2008, 012017.
15. **STMicroelectronics, (2015).** http://www.st.com/web/en/catalog/mmc/FM141/SC1169.
16. **Graham, B.M. (2007).** Enhancements in Electrical Impedance Tomography (EIT) Image Reconstruction for 3D Lung Imaging. PhD dissertation, University of Ottawa.
17. **Achmad, A., Prawito, P., Sastra, K.W. (2018).** Design and development of electrical impedance tomography system with 32 electrodes and microcontroller.
18. **Singh, G., Anand, S., Lall, B., Srivastava, A., Singh, V. (2015).** Development of a microcontroller based electrical impedance tomography system, Long Island Systems,

Applications and Technology. Farmingdale, pp. 1–4.

19. **Benetti, R., Cavalheiro, A.C.M., Nasiri, H., Takimoto, R.Y., Duran, G.C., Ueda, E.K., Ferro, R.A.O., Barari, A., Martins, T.C., Tsuzuki, M.S.G. (2023).** Electrical Impedance Tomography Hardware with Demodulation. IFAC-PapersOnLine, Vol. 56, No. 2.

Article received on 29/08/2024; accepted on 13/01/2025.
**Corresponding author is Miguel Ángel San-Pablo-Juárez.*